A Compact Low Profile Modified ACS-fed Triple Band Open-Ended Metamaterial Antenna for UMTS, WLAN, and WiMAX Applications

Mohammad Ameen*[(1)], Sachin Kalraiya[(2)], and Raghvendra Kumar Chaudhary[(3)]
Department of Electronics Engineering, Indian Institute of Technology (Indian School of Mines), Dhanbad, Jharkhand, India
[(1)]mohammadmn61@gmail.com, [(2)]sachinkalraiya12@gmail.com, and [(3)]raghvendra.chaudhary@gmail.com

Abstract

A new, compact and low profile triple band metamaterial (MTM) antenna based on the open-ended configuration of composite right/left-handed (CRLH) transmission line (TL) is discussed in this paper. The intended antenna obtains a compact size (ka = 0.8 <1) due to its zeroth order resonance (ZOR) property with an overall electrical dimension of 0.16 λ_0 × 0.19 λ_0 × 0.004 λ_0 at 2.16 GHz and an overall antenna dimensions of 23 × 27 × 0.6 mm^3. The antenna covers three resonances from (2.14–2.18 GHz), (3.14–3.65 GHz), and (4.59–7.34 GHz) frequency bands with -10 dB S_{11} bandwidths of 1.85%, 15.22%, and 49.10% for the three frequency bands. The intended MTM antenna provides an average gain of 2 dBi, 1.2 dBi, and 4 dBi respectively for the three resonances. Measured S_{11} shows almost similar result with the simulated result demonstrates that the intended triple band MTM antenna is appropriate for working in the 2.2 GHz UMTS, 3.6/5.2/5.8 GHz WLAN, and 3.3/3.5/5.5 GHz WiMAX applications.

1. Introduction

Multiple band compact antennas with multifunctionality are needed for the future wireless communication systems due to the day to day technology advancements. If a single antenna can provide more than one bands with multiple characteristics can save the cost and solve space constraint problems faced by the conventional microstrip antennas. Traditional microstrip antennas fail to provide wider bandwidth with compact size what the current application systems needed. One of the major breakthroughs was the introduction of metamaterials (MTMs). MTMs are artificial homogenous structures, which have simultaneously both permeability (μ) and permittivity (ε) will be negative. These properties are shown by the left-handed (LH) materials with various unusual characteristics which are not obtainable by conventional right-handed materials [1]–[2]. A variety of MTM based antennas are explained in [1]–[9]. Several types of multiband MTM antennas are explained in the literature which uses CRLH-TL MTM [1, 3], complementary capacitive loops [4], CRLH-TL with double hexagonal SRR [5], closed ring resonator [6], ELC and EBG loading [7], MTM loading [8] and MTM inspired structures [9] for multiband and compactness. Even though these antennas facilitate moderate bandwidth, but they are not providing compactness and gain required for the current technology demands. Current antenna designs are focusing towards miniaturization.

In this paper, a compact and low profile tri-band MTM based antenna by utilizing the open-ended boundary condition of CRLH-TL. The intended triple band antenna provides wider bandwidth and good gain with lesser size. The results of the designed antenna are compared with currently existing tri-band MTM antenna designs found in the literature. All the simulations and their corresponding results are based on CST microwave studio.

2. Antenna Geometry and Design

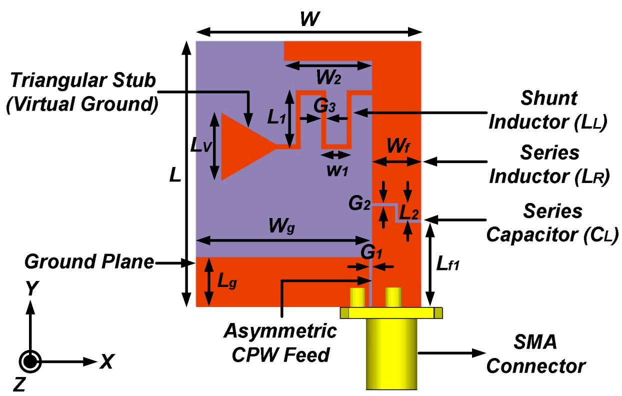

Figure 1. Simplified view of the intended tri-band linearly polarized antenna with dimensions.

The schematic diagram of the intended tri-band LP MTM antenna with dimensions are marked as described in Figure 1. The intended MTM antenna structure is fabricated on FR-4 substrate with a height of h = 0.6 mm, relative permittivity (ε_r) 4.4, and loss tangent ($tan\ \delta$) of 0.02. Asymmetric coplanar strip (ACS) feeding is used in this antenna for antenna miniaturization. The advantage of this design is that the radiating MTM antenna and ground plane are located on the same plane of the substrate. So, the fabrication process is very easy. The antenna consists of an inverted 'L' shaped feed line of width (W_f)and length (L_{f1} + L_2+ L_{f2}+ W_2). A step type slot of width G_2 is inserted in the feed line itself, which provides the series capacitance (C_L) of CRLH-TL. A meander line (for realizing shunt parameters L_L and C_R) is connected with the feed line and it is terminated with a triangular shaped stub (virtual ground). The total dimensions of the intended MTM antenna are 23 mm × 27 mm× 0.6 mm with electrical size of 0.16 λ_0 × 0.19 λ_0 × 0.004 λ_0 at 2.16 GHz. The optimized dimensions are L = 23 mm, L_1 = 6 mm, L_2 = 1.7 mm, L_V = 6.92 mm, L_{f1} = 8.5 mm, L_{f2} = 18.20, L_g = 5 mm, W = 27 mm, W_1 = 1.8 mm, W_2 = 9 mm, W_g = 17.7 mm, W_f = 5 mm, G_1 = G_2 = 0.3 mm, G_3 = 0.5 mm.

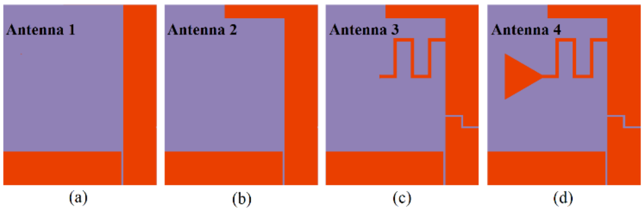

Figure 2. Antenna design stages for the generation of triple band characteristics.

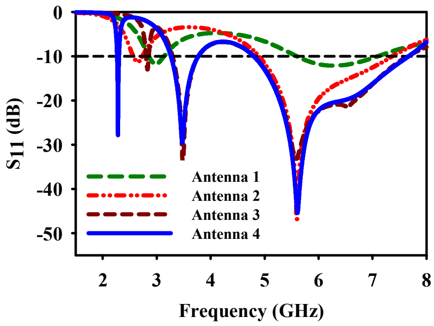

Figure 3. Input reflection coefficient (S_{11}) responses of the intended MTM antenna at different design stages described in Figure 2.

Figure 2 and Figure 3 shows the evolution of the antenna design and its reflection coefficient characteristics (S_{11}). At first, a simple microstrip line feed with an asymmetric ground plane the top side which is denoted as Antenna 1. The extension of the feed line and converted to an inverted L shaped feed represented as Antenna 2. Addition of CRLH-TL without triangular stub represented as Antenna 3, and the final optimized antenna denoted as Antenna 4.

3. Equivalent Circuit Model of the Designed MTM Antenna

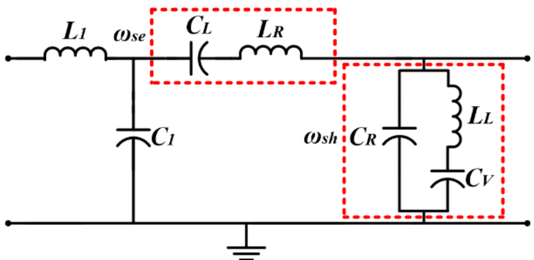

Figure 4. Equivalent circuit representation for the intended tri-band MTM antenna.

The intended tri-band MTM antenna depicted in Figure 1 is based on open-ended boundary condition of CRLH-TL transmission line. The equivalent circuit representation of the antenna is described in Figure 4. In the circuit model, consists of a series inductor (L_1) which is due to the L_{f1} × W_f part of the feedline, the gap connecting between the feedline and asymmetric ground plane represented by shunt capacitor (C_1). Series capacitance (C_L) is due to the step type slot, series inductance (L_R) is due to L_{f2} × W_f part. Shunt inductance (L_L) is due to the meander lines, and shunt capacitance (C_R) is due to the gap between the meander lines. An extra capacitor (C_V) due to the coupling between the triangular stub and the modified ACS ground plane. Here the triangular stub working as a virtual ground. The resonant frequency (f_{ZOR}) of the intended open-ended MTM based antenna is controlled by the lumped values of shunt elements. The ZOR frequency is given by (1),

$$f_{ZOR} = \frac{1}{2\pi\sqrt{L_L\left(\frac{C_V\,C_R}{C_V + C_R}\right)}} \qquad (1).$$

Figure 5 depicts the variation of the reflection coefficient by changing the width of the series capacitor (C_L). It is observed that when the width G_2 is changing from 0.1 mm 0.9 mm there is no change in the ZOR frequency. But in the case of second resonance, a small shift is introduced. There is no change in the third resonance. Similarly, Figure 6 shows the variation of the shunt capacitor (C_R) by changing the width (W_1). It is clearly observed that the variation of shunt parameter, ZOR is changing and an optimum value of W_1 = 1.8 mm is chosen. There is no change in the second and third resonances.

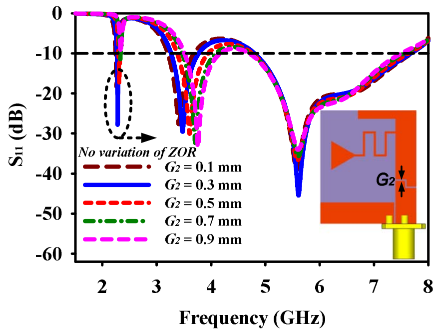

Figure 5. Input reflection coefficient (S_{11}) responses of the antenna by varying the gap G_2 of the series capacitor (C_L).

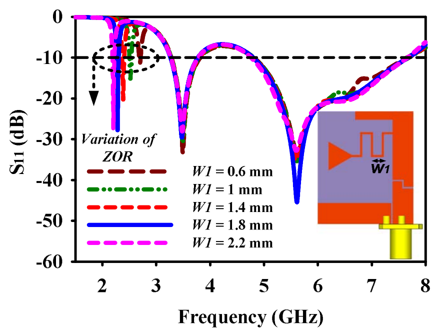

Figure 6. Input reflection coefficient (S_{11}) responses of the antenna by varying the gap W_1 of the shunt capacitor (C_R).

Figure 7 shows the variation of shunt inductor (L_L) by changing the meander line length L_1. It is observed that increasing the meander line length L_1 resonance will shift to a lower frequency, indicating the increment of shunt inductance (L_L) and an optimum value of L_1 = 6 mm is chosen. So it is confirmed that the variation of shunt parameters, there is a shift in the frequencies and no shift is observed in the case of varying series elements. So it is proved (eqn. (1)) that the variation of shunt parameters will lead to the generation of ZOR.

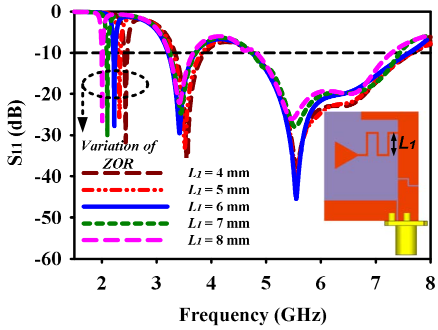

Figure 7. Input reflection coefficient (S_{11}) responses of the antenna by varying the length L_1 of the shunt inductor (L_L).

4. Results and Discussions

The photograph of the fabricated model is depicted in Figure 8. To validate the simulation results of CST, the reflection coefficient (S_{11}) are measured by the N9925A vector network analyzer. The measured 10-dB bandwidths for the triple-band antenna is 40 MHz (2.14–2.18 GHz), 510 MHz (3.14–3.65 GHz), and 2759 MHz (4.59–7.34 GHz) corresponding to fractional bandwidths of 1.85%, 15.22%, and 49.10% for the three bands corresponding to center frequencies of 2.16 GHz, 3.35 GHz, and 5.6 GHz respectively as displayed in the Figure 9.

Figure 8. Fabricated prototype of the intended tri-band MTM antenna.

The radiation behavior of the intended antenna is also examined. Figure 10 displays the simulated 2-D radiation patterns in *yz*–plane and *xz*–plane of each band at 2.2 GHz, 3.5 GHz, and 5.6 GHz respectively. For the case of *xz*–plane at three frequencies bidirectional radiation pattern is noticed and in *yz*–plane good omnidirectional pattern is noticed. Cross polarization is higher in 3.5 GHz due to the close arrangement of *E*-field inside the antenna due to the low profile and compactness nature of the intended antenna.

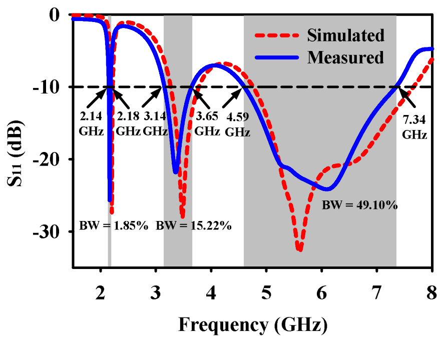

Figure 9. Measured and simulated S_{11} response of the intended tri-band MTM antenna.

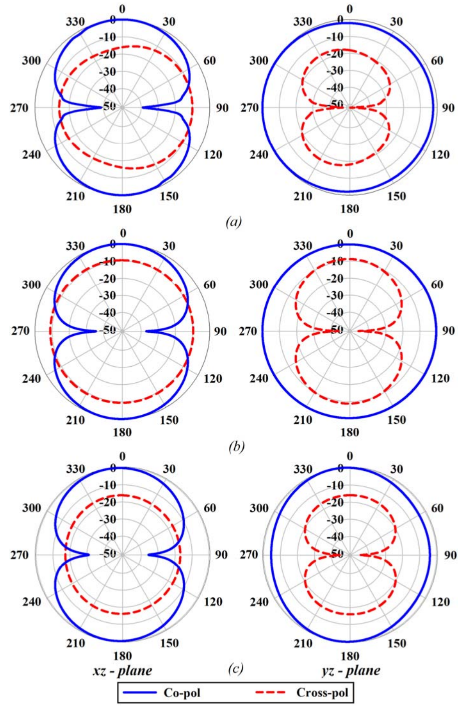

Fig. 10. Simulated radiation pattern of the intended MTM antenna (a) 2.2 GHz, (b) 3.5, and (c) 5.6 GHz.

Figure 11 depicts the gain and radiation efficiency for the MTM antenna. The antenna provides a gain of (1.78–2.07 dBi), (1.11–1.52 dBi) and (3.8–4.51 dBi) with an average gain of 2 dBi, 1.2 dBi, and 4 dBi for the three consecutive bands respectively. The radiation efficiency of the antenna also plotted. An efficiency of 73.74%, 96.2%, and 98.5% is observed for the three consecutive bands respectively.

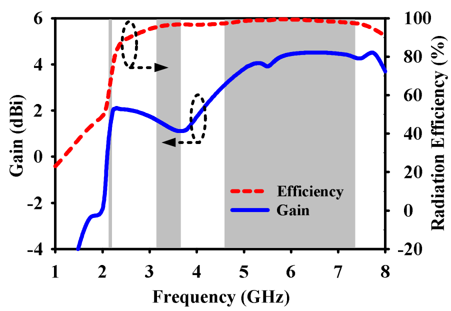

Figure 11. Simulated gain and radiation efficiency of the intended MTM antenna.

Table 1. Comparison between the intended MTM antenna and existing triple band MTM antennas

Ref. No.	Freq. (GHz)	Antenna Size (mm)	Electrical size (λ_0)	*Ka* value	Impedance BW (%)	Gain (dBi)	Type	Applications
[4]	2.5	70 × 78.5 × 0.8	0.58 × 0.64 × 0.006	2.7	22	1.4	Microstrip	WLAN, WiMAX
	3.5				17	3.85		
	5.5				17	4.55		
[5]	2.61	28 × 20 × 1.6	0.17 × 0.24 × 0.013	0.94	6.54	2.4	CPW	WLAN, WiMAX
	4.12				6.61	3.38		
	6.24				34.20	4.26		
[6]	2.08	40 × 45 × 1.6	0.315 × 0.280 × 0.011	1.31	5.76	1.87	Microstrip	WLAN, LTE, CDMA
	4.31				1.40	2.90		
	5.50				2	4.13		
[7]	2.5	35 × 35 × 1	0.29 × 0.29 × 0.008	1.29	2.4	NA	Microstrip	WLAN, WiMAX
	3.5				19.42	NA		
	5.5				18.36	NA		
[8]	2.45	20 × 23.5 × 1.59	0.16 × 0.19 × 0.013	0.77	3.6	1.14	CPW	WiFi, WiMAX
	3.5				17.71	1.15		
	5.5				32.72	1.78		
[9]	1.78	20 × 20 × 0.508	0.11 × 0.11 × 0.003	0.52	3.08	-0.15	CPW	Not specified
	4.22				15.17	2.18-3.58		
	5.8				8.33	2.18-3.58		
Proposed Antenna	**2.16**	**23 × 27 × 0.6**	**0.16 × 0.19 × 0.004**	**0.80**	**1.85**	**1.78-2.07**	**ACS**	**UMTS, WLAN, WiMAX**
	3.35				**15.22**	**1.11-1.52**		
	5.6				**49.10**	**3.8-4.51**		

Note: The electrical size of some antenna configurations in the above table is determined on the basis of their corresponding wavelength. Some papers, electrical size, *ka* value, and overall antenna size are not directly given and they are calculated according to the presented antenna designs.

5. Conclusion

A compact, low profile and triple band MTM antenna is designed and analyzed. The antenna provides bandwidths of 1.85%, 15.22% and 49.10% for the three bands respectively. Equivalent circuit diagram and parametric analysis are conducted for proving the MTM behavior. The antenna achieves a miniaturized size of 0.16 λ_0 × 0.19 λ_0 × 0.004 λ_0 with $ka = 0.8 < 1$, which can be easily integrated with current low profile wireless applications. The antenna can work in the 2.2 GHz UMTS, 3.6/5.2/5.8 GHz WLAN, and 3.3/3.5/5.5 GHz WiMAX application bands.

6. Acknowledgements

This research work is supported by Science and Engineering Research Board (SERB), DST, Government of India under grant number EEQ/2016/000023.

7. References

1. J. Lee, W. Huang, A. Gummalla, and M. Achour, “Small Antennas Based on CRLH Structures: Concept, Design, and Applications,” *IEEE Antennas and Propagation Magazine,* **53**, 2, April 2011, pp. 10-25, doi: 10.1109/MAP.2011.5949321.

2. M. Ameen, and R. K. Chaudhary, “Metamaterial-based circularly polarised antenna employing ENG-TL with enhanced bandwidth for WLAN applications,” *Electron. Lett.*, **54**, 20, October 2018, pp. 1152–1154, doi: 10.1049/el.2018.5701.

3. H. M. Lee, “A compact Zeroth-Order Resonant Antenna Employing Novel Composite Right/Left-Handed Transmission-Line Unit-Cells Structure,” *IEEE Antennas and Wireless Propag. Lett.*, **10**, December 2011, pp. 1377–1380, doi: 10.1109/LAWP.2011.2177798.

4. L. M. Si, Q. L. Zhang, W. D. Hu, W. H. Yu, *et al.*, “A Uniplanar Triple-Band Dipole Antenna Using Complementary Capacitively Loaded Loop,” *IEEE Antennas and Wireless Propag. Lett.*, **14**, March 2015, pp. 743–746, doi: 10.1109/LAWP.2015.2396907.

5. M. Ameen, R. Kumar, N. Mishra, and R. K. Chaudhary, “A Compact Triple Band Dual Polarized Metamaterial Antenna Loaded With Double Hexagonal SRR for WLAN/WiMAX Applications,” *iAIM*, November 2017, doi:10.1109/IAIM.2017.8402518.

6. A. Gupta, and R. K. Chaudhary, “A Compact Planar Metamaterial Triple-Band Antenna With Complementary Closed-Ring Resonator,” *Wireless Personal Comm*, **88**, 2, May 2016, pp. 203–210.

7. K. Li, C. Zhu, L. Li, Y. M. Cai, and C. H. Liang, “Design of Electrically Small Metamaterial Antenna with ELC and EBG Loading,” *IEEE Antennas and Wireless Propag. Lett.*, **12**, May 2013, pp. 678–681, doi: 10.1109/LAWP.2013.2264099.

8. J. Zhu, M. A. Antoniades, and G. V. Eleftheriades, “A Compact Tri-Band Monopole Antenna with Single-Cell Metamaterial Loading” *IEEE Trans. Antennas Propag.*, **58**, 4, April 2010, pp. 1031–1038. doi: 10.1109/TAP.2010.2041317.

9. N. Amani, M. Kamyab, A. Jafargholi, *et. al*, “Compact Tri-Band Metamaterial-Inspired Antenna Based on CRLH Resonant Structures,” *Electron. Lett.*, **50**, 12, June 2014, pp. 847–848, doi: 10.1049/el.2014.0875.